Self-Assembling Mn-Based Nanostructures

A. Bonanni, H. Seyringer, K. Hingerl, and H. Sitter

Institut für Halbleiterphysik, Johannes Kepler Universität, A-4040 Linz

D. Stifter

Profactor GmbH, Wehrgrabengasse 5, A-4040 Steyr

We report on the fabrication, by means of molecular beam epitaxy, of Mn-based nanostructures on CdTe and on the possibility to obtain regular islands with different morphology during the subsequent deposition of semiconductor compounds. The processes are monitored in situ and in real time via reflectance difference spectroscopy.

1. Introduction

In the area of semiconductor materials, self-assembling nanostructures [1] are attracting considerable attention because of their potential applications in electronic and optoelectronic devices as e.g. single electron transistors and quantum dot lasers. CdTe-based semiconducting magnetic heterostructures (MH), both in the diluted semimagnetic (DMS) phase of $Cd_{1-x}Mn_xTe$ [2] and in the digital (DMH) arrangement embedding MnTe magnetic layers [3], [4], offer the unique opportunity of having electronic band structures which can considerably be tuned by the application of magnetic fields of moderate intensity [5], [6]. In addition, the introduction of magnetic clusters in a semiconducting matrix opens new perspectives for applications in spin-dependent switching devices and in storage technology [7]. Puzzling morphologies of self-assembled islands, depending on the growth conditions and due to strain and stress effects [8], [9] and surface diffusion processes, could represent, when properly controlled, interesting new systems for electronic confinement in low dimensions. In addition, with the presence of magnetic elements, they could allow for the study of non-collinear magnetic structures' formation [10] and of strain effects on magnetic phases. In the present work, we essentially focus on the formation of pure Mn nanocrystallites on CdTe and then on the possibility to obtain regular islands with different morphology during the subsequent deposition of semiconductor compounds.

2. Experimental

All structures are fabricated by molecular beam epitaxy (MBE) on GaAs(001)-oriented substrates: a 0.5 µm thick CdTe buffer layer is at first deposited in excess of Te at a substrate temperature of 280 °C. The subsequent heteroepitaxy leading to island formation is carried out on the 2x1 Te-terminated CdTe(001)-oriented surface, keeping the substrate temperature constant. The MBE system is equipped with a reflection high energy electron diffraction (RHEED) apparatus with 20 keV operating voltage, suitable to follow changes in the surface reconstruction during the growth process.

With the aim of making the various formation stages reproducible, we follow the deposition phases via *in-situ* reflectance difference spectroscopy (RDS): this real-time technique allows to measure the difference between normal-incidence reflectances for light polarized along the two principal axes of the surface and it can be considered as a normal incidence ellipsometry, sensitive to surface and interface anisotropies [11], [12]. For the (001)-oriented surface we are interested in, symmetry considerations show that the optical eigenstates are $[\bar{1}10]$ and [110], thus the complex reflectance coefficients for light polarized along these axes are $r_{\bar{1}10}$ and r_{110}. The parameter measured is the relative difference: $\Delta r/r=(r_{\bar{1}10}-r_{110})/[(r_{\bar{1}10}+r_{110})/2]$. Our *in-situ* RDS system is similar to the one reported in [13]. In our study, we consider the real-time kinetic mode of RDS, where $\Delta r/r$ is monitored as a function of time. All data are acquired at the fixed energy of 3.26 eV, corresponding to the E_1 electronic transition for CdTe at the considered temperature.

By following the growth process simultaneously by means of RDS in kinetic mode and RHEED, we are able to detect the significant phases of islands' formation and to obtain the reproducibility of the structures. After major changes in RDS kinetics (Fig.1), the growth process is interrupted and the surface morphology examined *ex-situ* via atomic force microscopy (AFM).

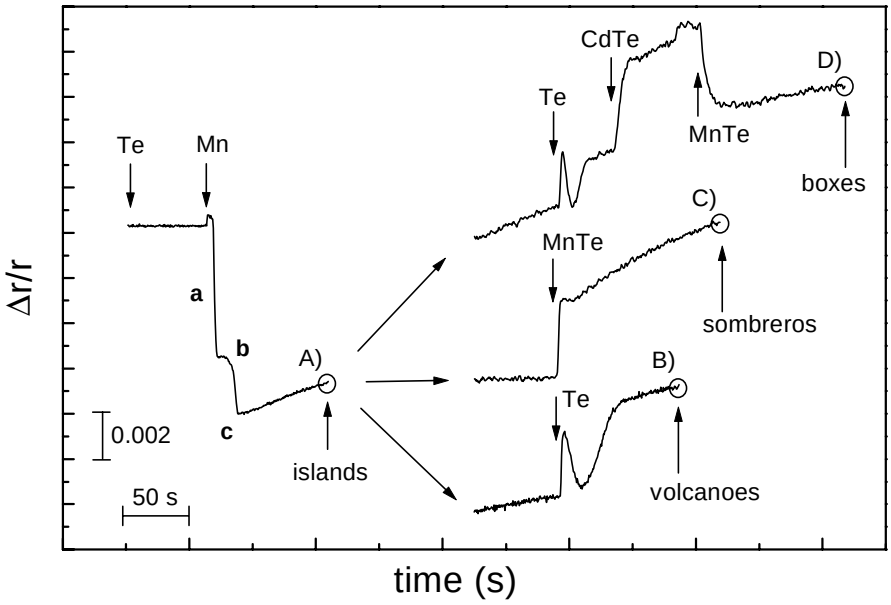

Fig. 1: Reflectance difference spectroscopy spectra in kinetic mode

The first step in our experiment is the deposition of pure Mn with a beam equivalent pressure of $0.3\text{x}10^{-8}$ Torr, on the Te-terminated CdTe(001) surface. As soon as the Mn nucleation starts, the RDS signal shows (region **a** in Fig.1(A)) an abrupt drop during the time corresponding to the growth of the first monolayer (ML). Successively (region **b** in Fig.1(A)), for the next two Mn MLs, the signal keeps constant, suggesting the formation of a wetting layer. After an additional steep decrease of the signal during the deposition of the fourth ML, we observe (point **c** Fig.1(A)) a sudden rise of the RDS signal and, simultaneously, a change in the RHEED pattern (till this moment stable at the 2x1 reconstruction typical for the Te-terminated CdTe surface): regular spots appear between the streaky features of the original reconstruction. From these facts we can infer that Mn

has been deposited in crystalline phase and with a lattice constant greater (smaller in the reciprocal crystallographic space mapped by RHEED) than CdTe. The surface morphology studied at this stage by means of AFM shows an arrangement of well defined islands like the one shown in Fig.2(A). For coverages from 6 to 15 MLs, we could distinguish a bimodal size distribution of nanocrystals with the smaller crystallites growing till a maximum of 20 nm in height and 150 nm in diameter and the bigger islands showing a narrow size distribution and an average height of 50 nm and average diameter of 200 nm. The average density on the surface is of 10 μm^{-2}. When we follow the same procedure described before, but instead of ending the growth after the formation of Mn islands, we proceed depositing Te, the evolution of RHEED pattern results in spots aligned along the 2x1 reconstruction with a distance corresponding to the lattice constant of MnTe. In addition, as soon as the Te deposition starts, the RDS signal produces an oscillation (Fig.1(B)) before saturating. By analyzing real ($\Delta r/r$) versus imaginary ($\Delta\theta$) part of the difference in anisotropy for the interval relative to the oscillation in $\Delta r/r$, we obtain a spiral-like trend (not shown), which is explained as the developing of a buried interface [14], in our case ascribed to diffusion of Te in Mn. AFM studies of the surface morphology at this stage, show 'volcanoes' (Fig.2(B)) with an average base diameter of 200 nm, a height of 20 nm, and cone-shaped craters with a maximum diameter of 50 nm. In this context, the effect can be explained in terms of strain induced by the presence of the Mn islands and having as a consequence the migration of adatoms along the side-walls of the crystallites and concomitant lack of dangling bounds in correspondence of the upper most region of Mn nanocrystals. We underline that the anti-dot-like shaped craters seem to be, because of morphology and size, promising candidates as hosts for 0-dimensional quantum structures.

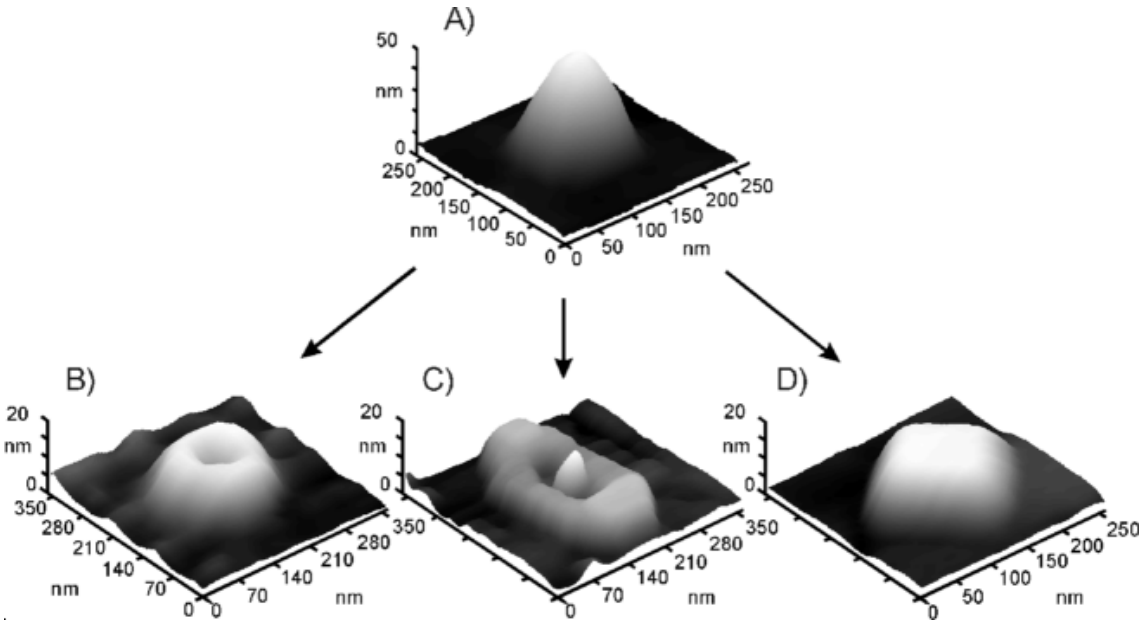

Fig. 2**:** AFM topographies.

In our search for different well controlled morphologies, we deposit 8 MLs of MnTe instead of pure Te on the precursor Mn crystallites (Fig.1(C)). After a Mn island is nucleated, the strain ε caused in the island by lattice mismatch is partially relaxed at the price of inducing an extra strain in the substrate and increasing the strain in the wetting

layer near the crystallite edge. Therefore, adatoms deposited on the wetted surface will have to overcome an energy barrier $\Delta\mu_s$ before they can attach to the island [15]. During successive growth, the evolution of the morphology is also influenced kinetically by surface stress, since adatoms tend to diffuse on the surface away from sites with high strain [16]. The strain concentration at the island edge increases monotonically with the island size; when it exceeds a critical value, the free energy for atoms to occupy a position at the island edge may become higher than that for atoms to occupy a crystallographically unusual, but less strained site [15]. These considerations explain why the growth of MnTe is hampered at the edges of the crystallites and tends to develop far from the borders of precursor Mn islands and generate the 'sombrero'-like features shown in Fig.2(C).

Finally, after the deposition of Te and successive 15 MLs of CdTe followed by 8 MLs of MnTe on the precursor Mn island (Fig.1(D)), we obtain a quasi-periodic arrangement of equally shaped 'boxes' with very regular squared bases of 200 nm x 200 nm and height of 20 nm (Fig.2(D)). Despite the presence of these features on the surface, the RHEED pattern appears streaky 2x1, due to the high density and the ML-scale flatness of the islands' top. The structures show the tendency to arrange along the [100] and [010] crystallographic directions, as predicted [17] for a stable array of islands on a (001)-oriented surface. Thermodynamic calculations have shown that after an island is nucleated the system free energy decreases monotonically with increasing island size [10]. Thus, a free energy minimum at a certain size is required in order to explain why observed islands' sizes tend to be so uniform. One should bear in mind not only the energetics, but also the kinetics, which implies that the islands' height grows slowly compared to the basis and may be treated as roughly constant. The kinetics can be incorporated by minimizing the total island energy with respect to width and length of the crystallite keeping the height constant. The result is that, in thermodynamic limit, with high density of islands, they should grow until each nanocrystal is square-based. This morphology represents the optimal trade-off between surface energy and strain. In our case the 'boxes', after reaching the squared-basis configuration, do not undergo further ripening and shape and basis size keep constant. Additional growth of MnTe leads to an increase of the crystallite height.

3. Conclusions

In conclusion, we achieved the reproducibility of self-assembling Mn-based nanocrystals, by monitoring in real time the subsequent stages of the growth process. The extension to other material systems and growth techniques would be straightforward, the RDS being suitable for MBE as well as for non-ultra-high-vacuum systems like chemical vapor deposition (CVD) reactors.

References

[1] D.Leonard, K.Pond, P.M.Petroff, *Phys. Rev. B* **50**, 11687 (1994).

[2] A.Haury, A.Wasiela, A.Arnoult, J.Cibert, S.Tatarenko, T.Dietl, Y.Merle d'Aubigné, *Phys. Rev. Lett.* **79**, 511 (1997).

[3] S.A.Crooker, D.A.Tulchinsky, J.Levy, D.D. Awschalom, R.Garcia, N.Samarth, *Phys. Rev. Lett.* **75**, 505 (1995).

[4] A.Bonanni, W.Heiß, G.Prechtl, D.Stifter, K.Hingerl, H.Sitter, *Phys. Stat. Sol. (a)* **164**, 331 (1997).

[5] H.Ulmer-Tuffigo, F.Kany, J.M.Hartmann, G.Feuillet, J.L.Pautrat, *Solid-State Comm.* **40**, 75 (1996).

[6] T.Mizokawa, A.Fujimori *Phys. Rev. B* **56**, 6669 (1997) and references therein.

[7] Jing Shi, S.Gider, K.Babcock, D.D.Awschalom, *Science* **271**, 937 (1996).

[8] J.Tersoff, F.K.LeGoues, *Phys. Rev. Lett.* **72**, 3570 (1994).

[9] W.Yu, A. Madhukar, *Phys. Rev. Lett.* **79**, 905 (1997).

[10] T.M.Giebultowicz, N.Samarth, H.Luo, J.K.Furdyna, P.Klosowski, J.J.Rhyne, *Phys. Rev. B* **46**, 12076 (1992).

[11] D.E.Aspnes, A.A.Studna, *Phys. Rev. Lett.* **54**, 1956 (1985).

[12] T.Jasuda, K.Kimura, S.Miwa, L.H.Kuo, C.G.Jin, K.Tanaka, T.Yao, *Phys. Rev. Lett.* **77**, 326 (1996).

[13] O.Acher, B.Drévillon, *Rev. Sci. Instrum.* **63**, 5332 (1992).

[14] B.A.Phillips, I.Kamiya, K.Hingerl, L.T.Florez, D.E.Aspnes, S.Mahajan, J.P.Harbison, *Phys. Rev. Lett.* **74**, 3640 (1995).

[15] Y.Chen, J.Washburn, *Phys. Rev. Lett.* **77**, 4046 (1996).

[16] Q.Xie, P.Chen, A.Madhrukar, *Appl. Phys. Lett.* **65**, 2051 (1994).

[17] V.A.Shuchukin, N.N.Ledentsof, P.S.Kop'ev, D.Bimberg, *Phys. Rev. Lett.* **75**, 2968 (1995).